

Short communication

Pore-forming agent induced microstructure evolution of freeze casted hydroxyapatite

Kai Hui Zuo^a, Yuan Zhang^{a,c}, Yu-Ping Zeng^{a,*}, Dongliang Jiang^{a,b}^a Shanghai Institute of Ceramics,

Chinese Academy of Sciences, Shanghai 200050, China

^b State Key Laboratory of High Performance Ceramics and Superne Microstructures, Shanghai Institute of Ceramics,
Chinese Academy of Sciences, Shanghai 200050, China^c Shanghai Research Institute of Building Sciences Co., Ltd., Shanghai 200000, China

Received 10 April 2010; received in revised form 22 April 2010; accepted 29 July 2010

Available online 21 August 2010

Abstract

There were interconnected small lamellar pores, big spherical pores and ceramic walls in the hydroxyapatite (HAP) ceramics fabricated by a freeze casting/pore-former method. As keeping the content of polymethyl methacrylate (PMMA) constant and decreasing the size of PMMA, the size of spherical pores and length of ceramic wall both decreased, and the compressive strength increased. As keeping the size of PMMA and decreasing the content of PMMA, the open porosity decreased and compressive strength increased. The shapes of pores caused by ice crystals were reticular, lamellar and treelike, in turn. The HAP ceramics with the spherical pores of 150–250 μm , open porosity of 62.13% and compressive strength of 7.01 MPa are prospective to have biomedical application.

© 2010 Elsevier Ltd and Techna Group S.r.l. All rights reserved.

Keywords: A. Drying; B. Porosity; C. Strength; E. Biomedical application

1. Introduction

Porous hydroxyapatite (HAP) becomes a promising ceramic material in biomedical application, such as artificial bone graft material and prosthesis revision surgery. To date, porous HAP ceramics have been prepared by various approaches, including conversion of natural bones, polymeric sponge method, gel casting of foams, slip casting, electrophoretic deposition technique and freeze casting [1–8]. Among them, freeze casting is a simple and effective way that can precisely control the pore structures (e.g., porosity, pore size and shape, connectivity of pores, and pore alignment) and improve mechanical properties by controlling the solid content of ceramics and freezing condition, etc. [7,8].

It is known that the interconnected pores with sizes of 50–500 μm are appropriate for the ingrowths of the surrounding bone [9–11]. Generally, the freeze casting method can fabricate interconnected pores; however, the size of pores obtained from this process is usually smaller than 50 μm . Thus, it is necessary

to develop effective methods to obtain large pores by freeze casting method. Recently, Yanase et al. reported that large pores can be fabricated by adding suitable pore-forming agents, such as polymethyl methacrylate (PMMA) [12]. So the freeze casting method with pore-former agent most likely fabricates interconnected pores larger than 50 μm .

In this work, porous HAP ceramics with controllable interconnected large pores were fabricated using freeze casting/pore-former method by fine tuning the size and content of PMMA, a pore-forming agent. The microstructures and mechanical properties of HAP ceramics were characterized.

2. Experimental materials and methods

HAP powder ($d_{50} = 0.4 \mu\text{m}$) was prepared by wet mechanic-chemical method with $\text{Ca}(\text{OH})_2$ (Analytical-grade, Shanghai Chemical Reagent Corp., China), $(\text{NH}_4)_2\text{HPO}_4$ (Analytical-grade, Shanghai Chemical Reagent Corp., China) and deionized water. The spherical PMMA particles (Shanghai Shanhu Chemical Reagent Corp., China) with mean sizes of 250–425 μm (symbol: PMMA-L), 150–250 μm (symbol: PMMA-M) and 75–150 μm (symbol: PMMA-S), were used as pore formers. Aqueous HAP slurry with initial solid loading of 50.0 wt% was

* Corresponding author. Tel.: +86 21 52415203; fax: +86 21 52413903.

E-mail address: yuping-zeng@mail.sic.ac.cn (Y.-P. Zeng).

prepared by mixing powder with a dispersant agent (ammonium polyacrylate, Bk Giulini, Germany) in deionized water. The slurry was ball-milled with ZrO_2 balls for 24 h. After that, PVA (Shanghai Chemical Reagent Corp., China) aqueous solution was used as a binder, and certain amount of PMMA was added into the slurry. The ratio of PVA to HAP powder is 2 wt% and the concentration of PVA aqueous solution is 12 wt%. The mixed slurry was ball-milled for another 24 h before freezing. The volume ratio of PMMA to HAP powder was set as 1, 2.3 and 4, respectively.

Then, the resultant slurries were poured into aluminum molds. All samples were frozen in a refrigerant under -18°C . After completely solidified, the samples were moved into a lyophilizer (TLG-A, Zhongke Biologic Co., Ltd, China) to dry. The drying time, temperature and pressure are 8 h, 60°C and 4 Pa, respectively. After freeze drying, the green bodies were heated to 550°C and held for 2 h to remove organic additives and sintered at 1300°C for 1 h in air. The sintered specimen of 1HAP-S ceramic means the specimen was fabricated using the slurry with PMMA-S and the volume ratio of PMMA to HAP powder was 1. The sintered specimen of 2.3HAP-L ceramic means the specimen was fabricated using the slurry with PMMA-L and the volume ratio of PMMA to HAP powder was 2.3.

The open porosity was measured by the Archimedes method in distilled water. The relative density is calculated by the measured density (ratio of weight to total volume) and theoretical density (3.16 g/cm^3). And the sum of relative density and total porosity is 1. The morphology of the sintered specimens was observed with scanning electron microscopy (SEM, JSM-6700F, JEOL, Akishima, Japan). The compressive strength of the sintered specimens was measured using Instron 5500R universal testing machine (Instron Ltd., Norwood, MA, USA) at a crosshead speed of 2.0 mm/min . The compressive loading was applied in the axial direction of sintered specimens. Four specimens were tested to obtain the average strength.

3. Results and discussion

3.1. Effect of the size of PMMA on the microstructures of porous HAP ceramics

Fig. 1 shows the micrographs of porous 2.3HAP ceramics with various sizes of PMMA adding. In all cases, they have small lamellar pores, large spherical pores and ceramic walls among pores. The spherical and lamellar pores are caused by decomposing of PMMA particles and sublimation of ice crystals, which are shown in Fig. 1(A) and (B), respectively.

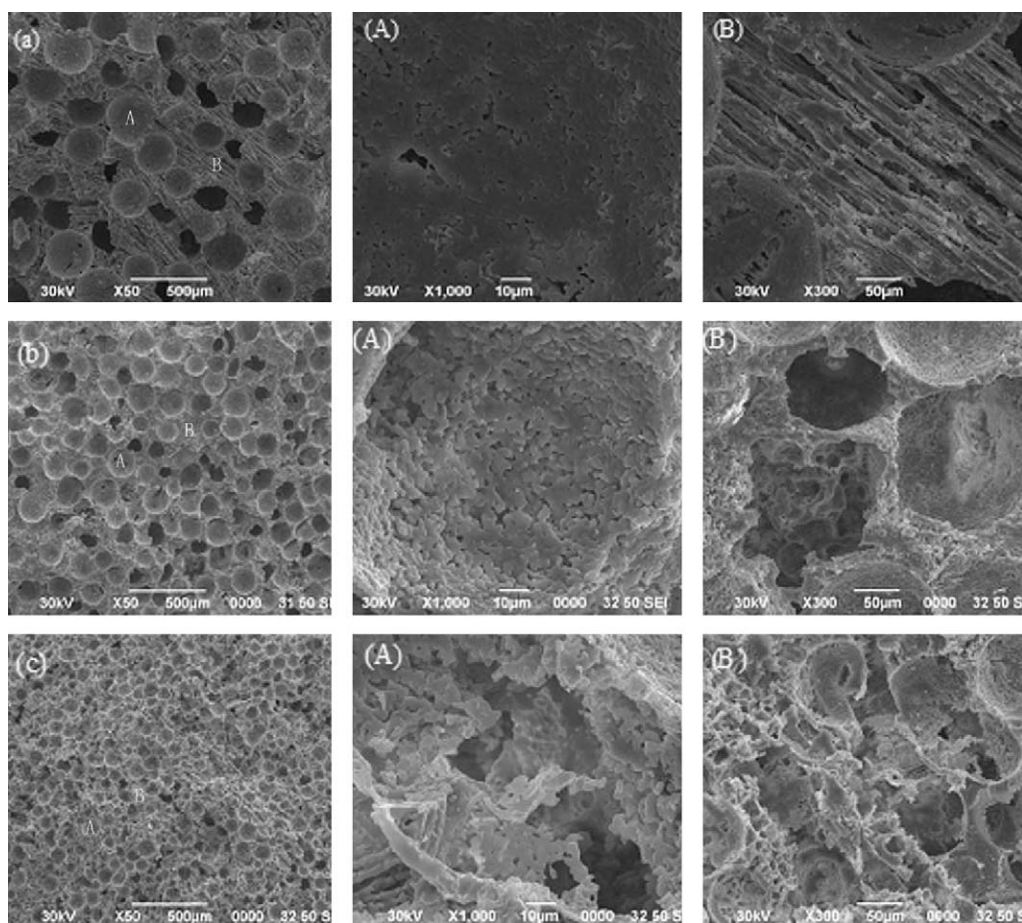


Fig. 1. SEM micrographs of the porous 2.3HAP ceramics, (a) 2.3HAP-L ceramic, (b) 2.3HAP-M ceramic, and (c) 2.3HAP-S ceramic. (A) and (B) show the wall of spherical pores caused by decomposing PMMA grains and pores caused by sublimation of ice crystals, respectively.

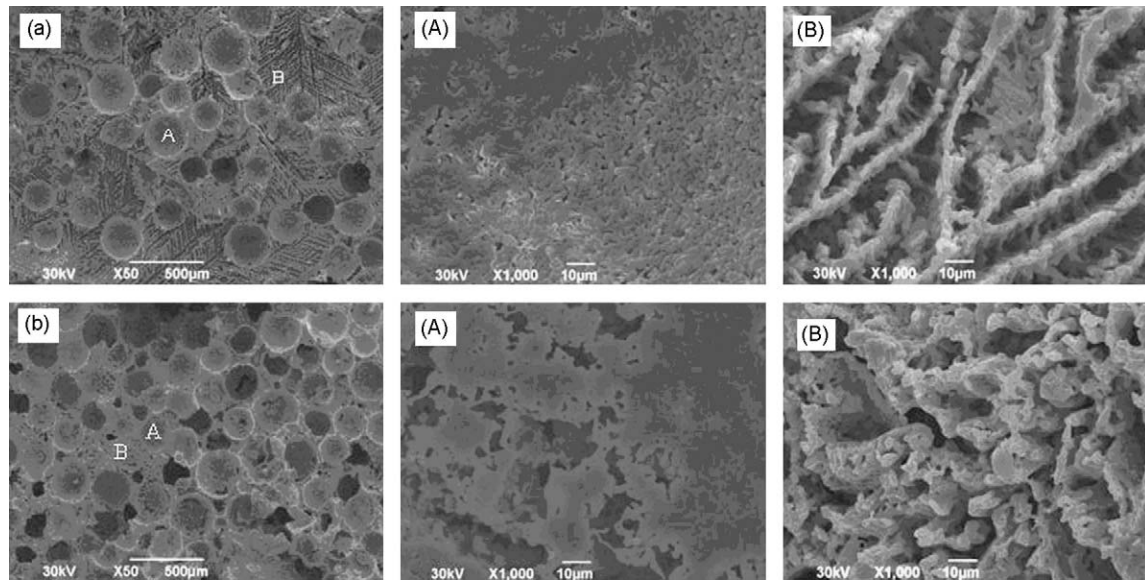


Fig. 2. SEM micrographs of the porous HAP-L ceramics, (a) 1HAP-L ceramic and (b) 4HAP-L ceramic. (A) and (B) show the wall of spherical pores caused by decomposing PMMA grains and pores caused by sublimation of ice crystals, respectively.

During freezing process, there are small lamellar ice crystals and ceramic walls enclosing PMMA grains which are squeezed out by ice crystals. Under a low pressure condition, the ice crystals sublimate, and then the lamellar pores and ceramic walls enclosing PMMA grains are obtained [13]. The decomposing temperature of PMMA is about 250–300 °C [12], thus spherical pores in the ceramic walls are easily obtained after sintered at 1300 °C. The sizes of the spherical pores of prepared ceramics are all larger than 100 μm and decrease if small PMMA particles are used. It can also be found from Fig. 1 that the distances between the lamellar pores decrease as decreasing the size of PMMA particles. Comparing the spherical pore of 2.3HAP-L ceramic with that of 2.3HAP-S ceramic, the compactness of pore's wall decreases with decreasing the size of PMMA, which means the connectivity of pores increases and this might be benefit for flowing and exchanging of nutritive materials. The reason for higher connectivity is that the small PMMA particles have larger surfaces areas, which have more probability to contact with HAP and PMMA particles.

3.2. Effect of the content of PMMA on the microstructures of porous HAP ceramics

Fig. 2 shows the micrographs of porous HAP-L ceramics with various contents of PMMA. Fig. 2(A) and (B) shows the

wall of spherical pores caused by decomposing PMMA grains and pores caused by sublimation of ice crystals, respectively. With increasing the content of PMMA, both the volume of spherical pores and the pore connectivity increase. Beside, the wall of spherical pores of 1HAP-L is denser than that of 4HAP-L ceramics. The pores from sublimation of ice crystals are treelike, lamellar and reticular in the 1HAP-L, 2.3HAP-L and 4HAP-L ceramics, respectively. The reason is that a large amount of PMMA causes more resistances to the growth of ice crystals. With increasing the resistances to the growth of ice crystals, the morphologies of ice crystals change into treelike, lamellar and reticular shapes. Fig. 2 also indicates the sizes of spherical pores of 1HAP-L and 4HAP-L ceramics are both larger than 200 μm .

3.3. Effect of the PMMA on the porosity and compressive strength of HAP ceramics

Table 1 lists the porosity, relative density and compressive strength of 2.3HAP ceramics with various sizes of PMMA and HAP-L ceramics fabricated with various contents of PMMA-L. First, for specimens with same content of PMMA, there is little difference in porosity. However, the compressive strength increases with decreasing the size of PMMA, which is caused by the decrease of the size of spherical pores and the length of

Table 1
Porosity and compressive strength of HAP ceramics fabricated with PMMA grains.

Specimens	Relative density (%)	Total porosity (%)	Open porosity obtained by Archimedes method (%)	Compressive strength (MPa)
2.3HAP-L	34.81	65.19	64.66	4.43 ± 0.19
2.3HAP-M	37.36	62.64	62.13	7.01 ± 0.03
2.3HAP-S	34.31	65.69	65.25	7.37 ± 0.08
1HAP-L	43.72	56.28	55.71	6.67 ± 0.14
4HAP-L	26.26	73.74	73.44	0.51 ± 0.03

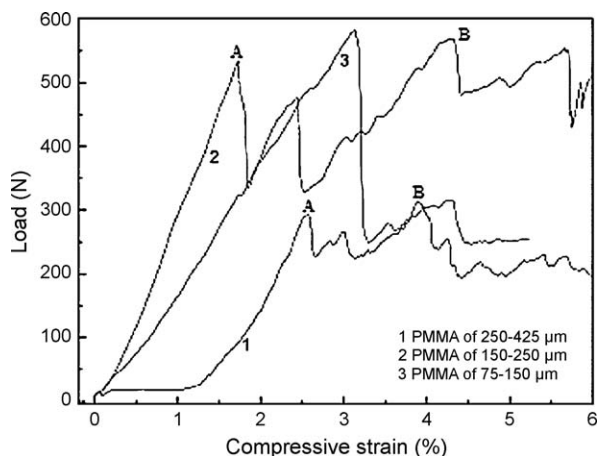


Fig. 3. Load vs strain diagrams of 2.3HAP ceramics with various sizes of PMMA.

ceramic walls. Table 1 also indicates that as increasing the content of PMMA-L, the porosity of HAP-L ceramics increases and compressive strength decreases. The 4HAP-L ceramic has the largest porosity of 73.43% and lowest fracture strength of 0.51 MPa. The 1PMMA-L ceramic has the smallest porosity of 56.28% and highest fracture strength of 6.67 MPa.

Fig. 3 shows the fracture curves of porous 2.3HAP ceramics with various sizes of PMMA. All specimens show the step-wise load behaviors, characterized of non-catastrophic fracture. After the outermost ceramic breaking (corroding to A point in curves), the subsequent load exceeds the breaking load, such as $\sigma_B > \sigma_A$, in cures of 2.3HAP-M and 2.3HAP-L ceramics (curves 1 and 2). However, this behavior does not happen in 2.3HAP-S ceramic (curve 3). This may be due to that the wall of pores in 2.3HAP-S ceramic has the loosest walls of pores, which can inhibit crack propagations.

4. Conclusions

In summary, the freeze casting/pore-forming agent method has been applied to fabricate porous HAP ceramics with interconnected large pores and good strength. Both of the size and content of PMMA affected the microstructures and properties of porous HAP ceramics. The sizes of the spherical pores caused by decomposing the PMMA grains are all larger than 100 μm and decrease if small PMMA particles are used. This method covers the shortage of the freeze casting method,

which only can fabricate ceramics with small pores and might have potential bio-applications.

Acknowledgements

The authors thank for the financial support from the National Natural Science Foundation of China (Project No. 50902140), Shanghai Committee of Science and Technology (Project 08JC1420300) and the support of Innovative Foundation of Shanghai Institute of Ceramics, Chinese Academy of Science.

References

- [1] S. Aoki, S. Yamaguchi, A. Nakahira, K. Suganuma, Preparation of porous calcium phosphates using a ceramic foaming technique combined with a hydrothermal treatment and the cell response with incorporation of osteoblast-like Cells, *J. Ceram. Soc. Jpn.* 112 (2004) 193–199.
- [2] D. Tadic, F. Beckmann, K. Schwarz, A novel method to produce hydroxyapatite objects with interconnecting porosity that avoids sintering, *Biomaterials* 25 (2004) 3335–3340.
- [3] S. Joschek, B. Nies, R. Krotz, A. Gopferich, Chemical and physicochemical characterization of porous hydroxyapatite ceramics made of natural bone, *Biomaterials* 21 (2000) 1645–1658.
- [4] N. Tamai, A. Myoui, T. Tomita, T. Nakase, J. Tanaka, T. Ochi, H. Yoshikawa, Novel hydroxyapatite ceramics with an interconnective porous structure exhibit superior osteoconduction, *J. Biomed. Mater. Res.* 59 (2002) 110–117.
- [5] J. Tian, J. Tian, Preparation of porous hydroxyapatite, *J. Mater. Sci.* 36 (2001) 3061–3066.
- [6] J. Ma, C. Wang, K.W. Peng, Electrophoretic deposition of porous hydroxyapatite scaffold, *Biomaterials* 24 (2003) 3505–3510.
- [7] T. Fukasawa, M. Ando, T. Ohji, S. Kanzaki, Synthesis of porous ceramics with complex pore structure by freeze-drying processing, *J. Am. Ceram. Soc.* 84 (2001) 230–232.
- [8] S. Deville, E. Saiz, R.K. Nalla, A.P. Tomsia, Freezing as a path to build complex composites, *Science* 311 (2006) 515–518.
- [9] B.S. Chang, C.K. Lee, K.S. Hong, H.J. Youn, H.S. Ryu, S.S. Chung, K.W. Park, Osteoconduction at porous hydroxyapatite with various pore configurations, *Biomaterials* 21 (2000) 1291–1298.
- [10] S.F. Hulbert, S.J. Morisson, J.J. Klawitter, Tissue reaction to three ceramics of porous and non-porous structures, *J. Biomed. Mater. Res.* 6 (1972) 347–374.
- [11] W. Frieb, J. Warner, in: F. Schuth, K.S.W. Sing, J. Weitkamp (Eds.), *Handbook of Porous Solids*, Wiley-VCH, Weinheim, 2002, p. 2923.
- [12] I. Yanase, Y. Ishikawa, S. Matsuura, H. Kobayashi, Effects of PMMA on porous structure of pollucite, *J. Eur. Ceram. Soc.* 26 (2006) 475–479.
- [13] K.H. Zuo, Y.P. Zeng, D.L. Jiang, Properties of microstructure controllable porous YSZ ceramics fabricated by freeze casting, *Int. J. Appl. Ceram. Technol.* 5 (2008) 198–203.